

A 90 GHz SINIS Detector With 2 GHz Readout

Aleksandra A. Gunbina[✉], Member, IEEE, Sumedh Mahashabde, Michael A. Tarasov[✉], Grigory V. Yakopov, Renat A. Yusupov[✉], Artem M. Chekushkin, Daria V. Nagirnaya, Sergey A. Lemzyakov, Vyacheslav F. Vdovin[✉], Member, IEEE, Alexei S. Kalaboukhov, and Dag Winkler[✉]

Abstract—A superconductor-insulator-normal metal-insulator-superconductor (SINIS) detector integrated in a planar 90 GHz band twin-slot antenna with a 2 GHz superconducting resonator readout was fabricated and experimentally studied. In order to achieve high pixel count, the traditional dc readout of the SINIS detector is replaced by NbN coplanar 13.850 mm long superconducting resonator. SINIS detectors have traditionally dc Junction Field Effect Transistor (JFET) room-temperature readout. Such readout requires individual wiring for each pixel, while the microwave readout is far less cluttered as only one coaxial line is needed for hundreds of devices. Such readout operates similar to frequency domain multiplexing (FDM) for microwave kinetic inductance detectors (MKID). The planar twin slot antenna has two parallel slots in a metal ground plane which are excited coherently by short sections of a coplanar waveguide (CPW) line with a SINIS detector at the center. One section of the CPW is extended past the slot in a long superconducting section which functions as a quarter wavelength resonator. This resonator is short circuited to the ground plane at the far end, with the expected open circuited end terminated by the SINIS detector in the antenna. We measured the response of sample to black body radiation temperatures 6 K and 9 K. The corresponding dynamic resistance maximum drops from 50 kΩ down to 30 kΩ. An RF readout channel comprising a coplanar coupler and a coplanar resonator has a resonant frequency of 1.8 GHz. Unloaded Q factor (without incoming irradiation) is 200.

The signal spectral characteristics and the response to the black body radiation have shown design values as expected.

Index Terms—SINIS detector, microwave readout, superconducting quarter-wavelength resonator.

I. INTRODUCTION

AT THE moment implementation of the terahertz band is one of the most quickly developing spheres with great prospects for different applications [1], such as astronomy, medicine, warfare, security systems, etc.

The astronomy projects set the most ambitious requirements to the parameters of receiving systems. So far the best results are to be seen in space-borne THz receivers. Such receivers are designed for studying cosmic microwave background (CMB) radiation and interstellar dust and gas clouds, or searching for possible variations of some fundamental constants. Such research is mainly related to experimental verification of modern cosmological theories. Many ground-based observatories already exist, as well as balloon and space missions for space exploration in this frequency range have been launched and being developed. As an example, such projects are ALMA [2],[3], South Pole Telescope [4],[5], OLIMPO [6], [7], Planck [8], [9], MILLIMETRON [10], [11], etc. The requirements set by those projects to modern receiving systems include a wide dynamic range and noise equivalent power (NEP) below 10^{-16} W/Hz $^{0.5}$ for ground-based observatories and 10^{-19} W/Hz $^{0.5}$ for space missions. At present the most advanced and widely used types of direct THz detectors are transition edge sensors (TES) [12], [13] and kinetic inductance detectors (KID) [14], [15]. TES have high sensitivity, but the dynamic range is narrow, rate is low, and operation requires high stability of the bath temperature. The main advantage of KIDs is a low level of intrinsic noise since the Nyquist noise does not occur, but the absolute value of the kinetic inductance response is relatively low. In the superconductor – insulator – normal metal – insulator –superconductor (SINIS) [16], [17] detectors the dynamic range is over 30 dB, responsivity approaches 10^9 V/W, and it is not so sensitive to variations of bath temperature.

One of the noise sources in such instruments is a readout system, which is the main problem of creating arrays with a large number of receiving elements (pixels). Readout systems with a large number of transistor amplifiers and with a large number of wires have a high level of intrinsic noise, which complicates the signal detection. SINIS detectors have traditionally room-temperature dc JFET-based readout. Such readout involve a lot of wiring down to the low temperature stage of

Manuscript received November 28, 2020; revised February 22, 2021; accepted March 20, 2021. Date of publication March 25, 2021; date of current version May 3, 2021. Manuscript receipt and acceptance dates will be inserted here. This work was supported in part by the Chalmers University of Technology by the Swedish Research Council (Vetenskapsrådet, under Project 2016-05256), and in part by the Knut and Alice Wallenberg Foundation. This work was carried out at the IREE RAS and IAP RAS within the framework of the state task and RFBR 19-52-80023 Project. The fabrication was carried out using USU 352529 facilities. The development of some elements of THz detectors and creating of some elements of experimental instruments for researching were made in the framework of RSF Project 19-19-00499. (*Corresponding author: Aleksandra A. Gunbina*.)

Aleksandra A. Gunbina and Vyacheslav F. Vdovin are with the Institute of Applied Physics, N. Novgorod 603155, Russia (e-mail: aleksandragunbina@mail.ru; vdovin@appl.sci-nnov.ru).

Michael A. Tarasov, Renat A. Yusupov, Artem M. Chekushkin, and Daria V. Nagirnaya are with the Kotelni-kov Institute of Radio Engineering and Electronics, Moscow 125009, Russia (e-mail: tarasov@hitech.cplire.ru; yusupovrenat@hitech.cplire.ru; chekushkin@hitech.cplire.ru; darianagirnaya@mail.ru).

Grigory V. Yakopov is with the Special Astrophysical Observatory, Nizhnij Arkhyz 369167, Russia (e-mail: yakopov@gmail.com).

Sergey A. Lemzyakov is with the Kapitza Institute for Physical Problems, Moscow 119334, Russia (e-mail: lemserj@gmail.com).

Sumedh Mahashabde, Alexei S. Kalaboukhov, and Dag Winkler are with the Chalmers University of Technology, SE41296 Göteborg, Sweden (e-mail: sumedh.mahashabde@chalmers.se; alexei.kalaboukhov@chalmers.se; dag.winkler@chalmers.se).

Color versions of one or more figures in this article are available at <https://doi.org/10.1109/TASC.2021.3068999>.

Digital Object Identifier 10.1109/TASC.2021.3068999

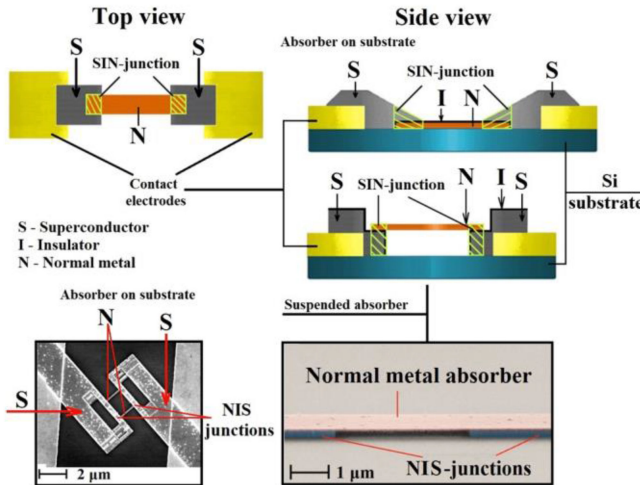


Fig. 1. Schematic image and SEM photos of different types of SINIS detector

the detector cryostat, while the microwave readout is far less cluttered with only microwave coaxial line for hundreds of devices. Accordingly, our research presented in this paper is focused on creating and testing a prototype of receiving structure based on a SINIS detector with a microwave readout system. We demonstrate the feasibility of such readouts, while their ultimate characteristics will be the matter of further research.

II. SINIS DETECTOR

The schematic image of a SINIS detector is presented in Fig. 1. The sensitive element of such detector is absorber made of normal metal typically around $1\mu\text{m} \times 100\text{ nm}$ with thickness of 15 nm. The radiation absorption in the SINIS structure leads to heating of the absorber, which can be measured as the tunnel current increase in the NIS thermometers. The nature of radiation absorption in such detectors has a complicated quantum character [18].

Typical characteristics of the SINIS detector with the JFET readout system are as follows:

- Responsivity – 10^9 V/W ;
- NEP – $10^{-16} \text{ W/Hz}^{0.5}$
- Detectors integrated in array are operable with a high background load [16], [17]
- Quantum efficiency - 15 electrons per quantum. High quantum efficiency can be achieved by fabricating a SINIS detector with a suspended absorber [18], [19]

III. MODELING

The schematic image of our model, which is a SINIS detector integrated in a planar 90 GHz band twin-slot antenna with a 13.85-mm long superconducting resonator is shown in Fig. 2(left). A planar twin-slot antenna (Fig. 2 right) has good directivity characteristics when used with a quasioptical horn or dielectric lens. This central frequency of 90 GHz was selected as we are planning to test the device at the BTA (Big Telescope Alt-azimuthal) [20], [21] where the atmospheric transparency above 100 GHz is poor. We have chosen this optical telescope

as it is the best instrument in Russia available for millimeter and sub-millimeter radio astronomy observations.

A. CPW Quarter-Wavelength Resonator

The resonant frequency of a quarter-wave resonator is determined by the Eqn. (1), where v_f is the phase velocity (Eqn. 2) and l is the resonator length.

$$F_{res} = v_f / 4l \quad (1)$$

$$v_f = \frac{1}{\sqrt{C \cdot L}} \quad (2)$$

C and $L = L' + L_{kin}$ are capacitance and inductance per unit length. C and L' can be calculated by using conformal mapping techniques [24]. L_{kin} is kinetic inductance calculated with Eqn. 3 from [25].

$$L_{kin} = \mu_0 \lambda_L(T) \cdot \left(\frac{C}{4ADK(k)} \right) \cdot \left[\left(\frac{1.7}{\sinh \left(\frac{t}{2\lambda_L(T)} \right)} \right) + \left(\frac{0.4}{\sqrt{\left[\left(\frac{B}{A} \right)^2 - 1 \right] \left[1 - \left(\frac{B}{D} \right)^2 \right]}} \right) \right] \quad (3)$$

where $K(k)$ is the elliptic integral, t - the film thickness and λ_L - London penetration depth (4):

$$\lambda_L(T) = \frac{\lambda_L}{\sqrt{\left[1 - \left(\frac{T}{T_c} \right)^4 \right]}} \quad (4)$$

The A-D parameters are calculated with the following equations from [25]:

$$A = -\frac{t}{\pi} + \frac{1}{2} \sqrt{\left(\frac{2t}{\pi} \right)^2 + g^2}; B = \frac{g^2}{4A}; \\ C = B - \frac{t}{\pi} + \sqrt{\left(\frac{t}{\pi} \right)^2 + w^2}; D = \frac{2t}{\pi} + C. \quad (5)$$

The calculated dependence of the resonant frequency on the operating temperature is shown in Fig. 3

The developed structure was modeled in CST STUDIO SUITE. We chose PEC (perfect electric conductor) for the material of the resonator. To take into account the additional kinetic inductance we used the additional lumped inductance. The modeled S21-parameter is shown in Fig. 4.

IV. FABRICATION TECHNOLOGY

The fabrication process of a sample includes two technology steps: firstly, formation of an NbN layer consisting of CPW, twin-slot antenna, conducting wires, and contact pads, and secondly, fabrication of the SINIS detector.

NbN layer (Fig. 5): The thin 50 nm film of NbN is sputtered on the high resistance silicon substrate. For formation of the resistive mask by e-beam lithography the UV5-0.8 resist was used. After developing the NbN film was etched in Cl_2/Ar plasma.

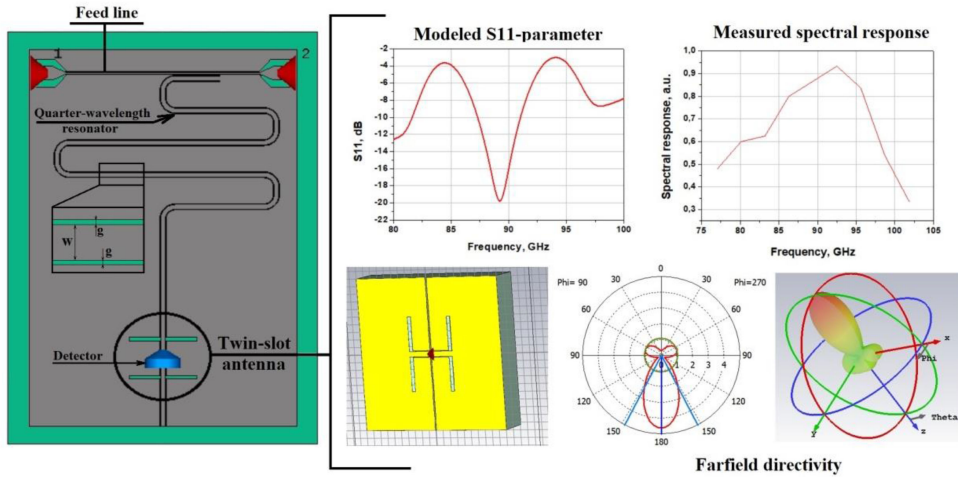


Fig. 2. The schematic image of modeled structure. Measured spectral response [22], [23].

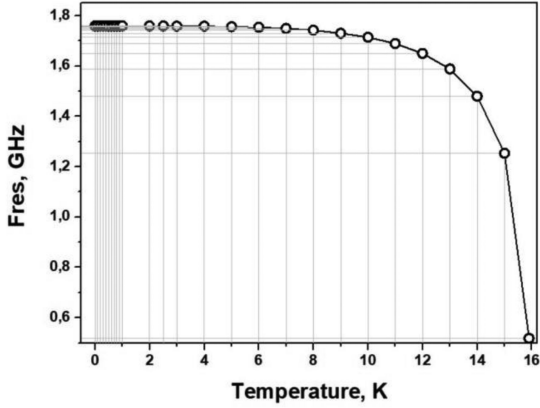


Fig. 3. Dependence of the resonant frequency on the operating temperature.

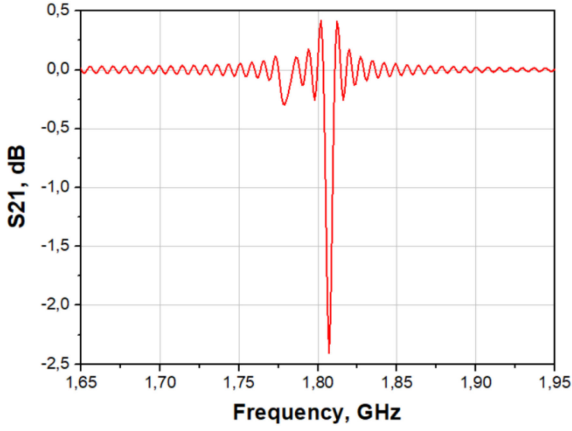


Fig. 4. Modeled S21-parameter in CST SUITE STUDIO.

Detector Fig. 6 [23], [26]: The bridge-free technology of the detector fabrication is shown in Fig. 6. The key element is to deposit separately two layers of different metals into two orthogonal deep grooves in a two-layer resist. While the deposition of the first film along the first groove film is not deposited into the orthogonal groove, since the deposition angle is chosen

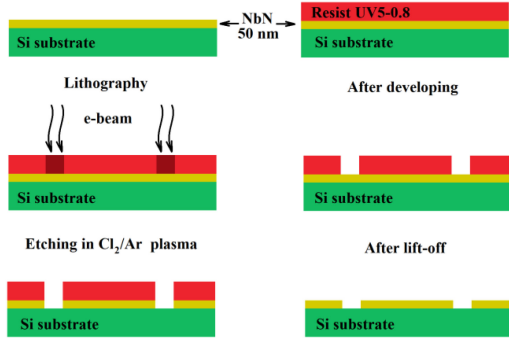


Fig. 5. The schematic image of fabrication of NbN layer.

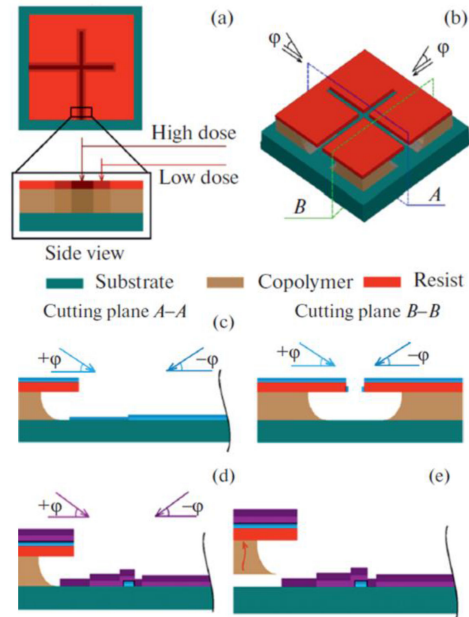


Fig. 6. The schematic image of bridge-free technology: The exposed structure: top view (a) and structure after developing in 3D-perspective (b),(c) – deposition of the first film (normal metal absorber –Fe/Al). After that, Al film is oxidized for formation of tunnel barrier. (d) – deposition of the second film (superconductor electrodes, Al); (e) – lift-off.

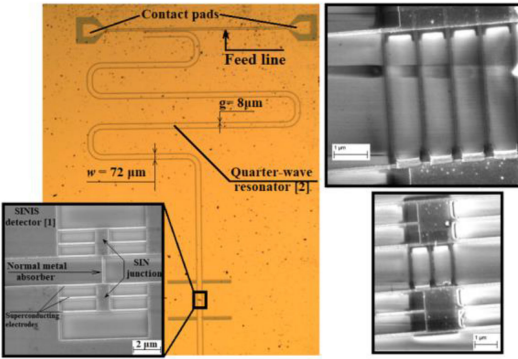


Fig. 7. Photos of fabricated sample.

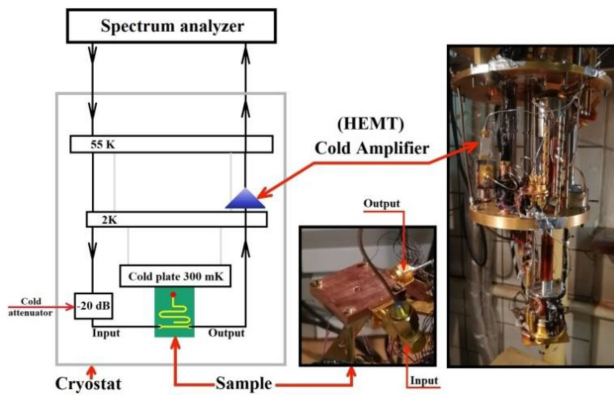


Fig. 8. The schematic image of experimental setup.

so that in the direction of the second groove, the deposition occurs on the resist wall with subsequent removal together with the resist. Similarly, when another film is deposited along the second orthogonal groove after rotation of the substrate by 90° around the axis, film is deposited only in the second groove.

The fabricated sample is shown in Fig. 7, left. For reducing the resistance of the absorber required to match the impedance of the antenna it is possible to make detectors with a number of parallel absorbers (example Fig. 7, right)

V. EXPERIMENTAL SETUP AND RESULTS OF MEASUREMENTS

The He3 refrigerator Heliox-AC-V by Oxford Instruments was used for cooling down the samples and the readout amplifier. The schematic image and photo of the experimental setup are shown in Fig. 8. A cold HEMT amplifier with circulator at the input was mounted on the plate with temperature of 2K and the sample holder on the cold plate with the operation temperature of 280 mK. We developed and made a special sample holder with two SMA connectors for testing different samples with the microwave readout system [22].

As the main objective, we measured S21-parameter (Fig. 9) at the operating temperature of about 300 mK. Also, the dependence of the resonant frequency on operating temperature was measured (Fig. 10). The dynamic resistance and response to the black body radiation with temperatures of 6 and 9 K were measured and presented in Fig. 11. The samples were fabricated during the same technological cycle as the samples from [22].

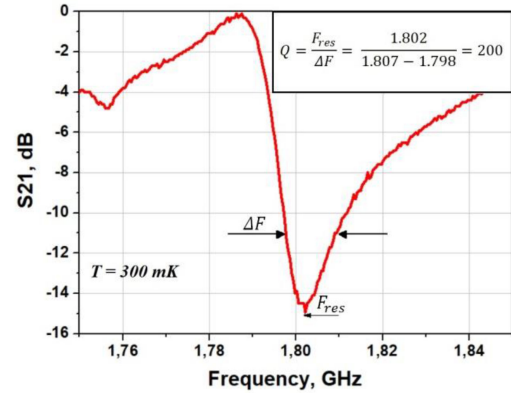


Fig. 9. The measured S21-parameter [dB].

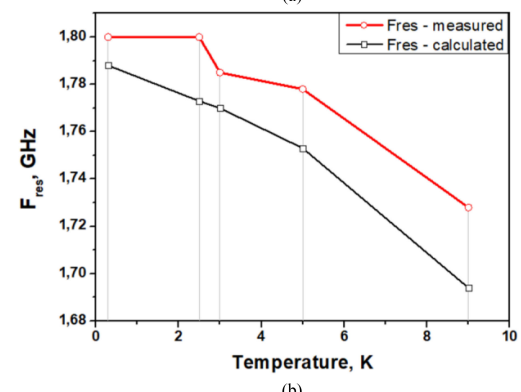
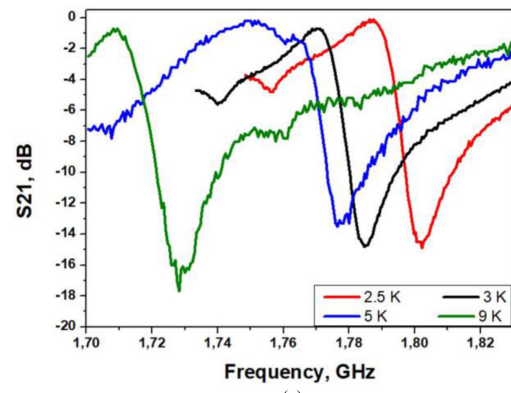


Fig. 10. Dependence of the resonant frequency on operating temperature: a - Measured S21-parameter; b -Comparison of calculated and measured resonant frequency.

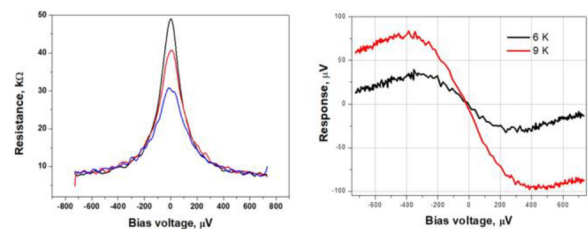


Fig. 11. Measured dynamic resistance (left) and Response to black body radiation (right). [11].

The measured characteristics of SINIS detectors are the same in both cases.

VI. CONCLUSION

A SINIS detector with microwave readout at resonant frequency of 1.8 GHz was designed, fabricated and experimentally studied. The spectral response was measured at a signal frequency in a frequency band of 90 GHz. The electrical response and dynamic resistance of such a bolometer at external radiation were measured at black body temperatures of 6 and 9 K. The dynamic resistance variates from 50 to 30 k Ω . The Q-factor of the readout resonator changes from 200 to 400. According to the obtained experimental data, we demonstrate that the SINIS detector can operate with a microwave readout system. The next step of our work is fabrication of SINIS detector matrix with different lengths of coplanar resonators on a single chip for separate readout via single coaxial.

ACKNOWLEDGMENT

The support from the Swedish Infrastructure for Micro- and Nanofabrication- Myfab is also appreciated.

REFERENCES

- [1] U. R. Pfeiffer. “Integrated circuit design for terahertz applications,” in *6G Wireless Summit*, Levi, Lapland, Finland, 2019.
- [2] [Online]. Available: <https://www.almabobservatory.org/en/home/>
- [3] R. L. Brown, W. Wild, and C. H. Cunningham “ALMA – the atacama large millimeter array,” *Adv. Space Res.*, vol. 34, no. 3, pp. 555–559, 2004.
- [4] [Online]. Available: <https://pole.uchicago.edu>
- [5] J. E. Carlstrom *et al.*, “The 10 meter south pole telescope,” *Pub. Astronomical Soc. Pacific*, vol. 123, no. 903, pp. 568–581, 2011.
- [6] [Online]. Available: <http://olimpo.roma1.infn.it>
- [7] G. Presta *et al.*, “The first flight of the OLIMPO experiment: Instrument performance,” *J. Phys.: Conf. Ser.*, vol. 1548, 2020, [Online]. Available: 10.1088/1742-6596/1548/1/012018
- [8] [Online]. Available: <https://www.cosmos.esa.int/web/planck>
- [9] P. A. R. Ade *et al.*, “Planck early results. I. The planck mission,” *Astron. Astrophys.*, vol. 536, 2011, [Online]. Available: <https://doi.org/10.1051/0004-6361/201116464>
- [10] [Online]. Available: <https://millimetron.ru/en/>
- [11] A. V. Smirnov *et al.*, “The current stage of development of the receiving complex of the millimetron space observatory,” *Radiophys. Quantum Electron.*, vol. 54, pp. 557–568, 2012, [Online]. Available: <https://doi.org/10.1007/s11141-012-9314-z>
- [12] P. Day *et al.*, “Distributed antenna-coupled TES for FIR detector arrays,” *J. Low Temp. Phys.*, vol. 151, pp. 477–482, 2008, [Online]. Available: <https://doi.org/10.1007/s10909-007-9676-3>
- [13] B. Westbrook *et al.*, “Development of the next generation of Multi-chroic antenna-coupled transition edge sensor detectors for CMB polarimetry,” *J. Low Temp. Phys.*, vol. 184, pp. 74–81, 2016, [Online]. Available: <https://doi.org/10.1007/s10909-016-1508-x>
- [14] P. K. Day *et al.*, “A broadband superconducting detector suitable for use in large arrays,” *Nature*, vol. 425, pp. 817–821, 2003, [Online]. Available: <https://doi.org/10.1038/nature02037>
- [15] A. Paiella *et al.*, “In-Flight performance of the LEKIDs of the OLIMPO experiment,” *J. Low Temp. Phys.*, vol. 199, pp. 491–501, 2020, [Online]. Available: <https://doi.org/10.1007/s10909-020-02372-y>
- [16] M. A. Tarasov *et al.*, “Arrays of annular antennas with SINIS bolometers,” *IEEE Trans. Appl. Supercond.*, vol. 30, no. 3, Apr. 2020, Art. no. 2300106, [Online]. Available: <https://doi.org/10.1109/TASC.2019.2941857>
- [17] M. Tarasov *et al.*, “Annular antenna array metamaterial with SINIS bolometers,” *J. Appl. Phys.*, vol. 125, no. 17, 2019, [Online]. Available: <https://doi.org/10.1063/1.5054160>
- [18] R. A. Yusupov *et al.*, “Quantum response of a bolometer based on the SINIS structure with a suspended absorber,” *Phys. Solid State*, vol. 62, no. 9, pp. 1403–1406, 2020, [Online]. Available: <https://doi.org/10.1134/S106378342009036X>
- [19] M. Tarasov *et al.*, “Electrical and optical properties of a bolometer with a suspended absorber and tunneling-current thermometers,” *Appl. Phys. Lett.*, vol. 110, no. 24, pp. 242601–1–242601–4, 2017, [Online]. Available: <https://doi.org/10.1063/1.4986463>
- [20] [Online]. Available: <https://www.sao.ru/Doc-en/Telescopes/bta/descrip.html>
- [21] G. Yakopov *et al.*, “SubTHz arrays of planar antennas with SINIS bolometers for BTA,” *EPI Web Conferences*, vol. 195, pp. 05014, 2018, [Online]. Available: <https://doi.org/10.1051/epjconf/201819505014>
- [22] M. A. Tarasov *et al.*, “SINIS bolometer with microwave readout,” *Phys. Solid State*, vol. 62, pp. 1580–1584, 2020, [Online]. Available: <https://doi.org/10.1134/S1063783420090292>
- [23] Yu. Yu. Balega *et al.*, Superconducting receivers for space, balloon and ground-based sub-THz radio telescopes. Submitted for publication, *Radiophys. Quantum Electron.*, vol. 63, no. 7, pp. 533–556.
- [24] C. Nguyen, “*Analysis Methods for RF, Microwave, and Millimeter-Wave Planar Transmission Line Structures*,” Wiley, 2000.
- [25] S. Hofmann/Design, *Fabrication and Characterization of a Microwave Resonator for Circuit QED: diploma thesis// Technical Univ. of Munich*. Munich, Mar. 2007.
- [26] M. Tarasov, A. Gunbina, D. Nagirnaya, and M. Fominskii, “Method of making device with thin-film tunnel junctions,” Patent Request No. RU2733330C1 20201001, 2019.